Towards Long-Term Solar Irradiance Modelling: Network Contrasts from Magneto-Convection Simulations

Y. C. Unruh*, S. K. Solanki†, M. Schüssler†, A. Vögler** and D. Garcia-Alvarez‡

*Astrophysics Group, Imperial College London, SW7 2AZ, U.K.
†Max-Planck Institut für Sonnensystemforschung, D–37191 Katlenburg-Lindau, Germany
**Astronomical Institute Utrecht, NL–3584CC Utrecht
‡Instituto de Astrofisica de Canarias, E–38205 La Laguna

Abstract. Solar irradiance changes on a wide range of time scales and is a key driver of the Earth's climate where secular variability in particular is relevant. This is, however, not well understood and our knowledge relies on reconstructions based on sunspot numbers and similar proxies.

The prime candidate to produce secular variability is a change in the surface coverage of small-scale magnetic elements. Direct observational determination of the flux emitted by these magnetic elements is difficult, especially as information covering a large spectral range is needed. Here we present a theoretical approach to this problem using intensity calculations from 3-D simulations of solar magneto-convection and compare these with the intensity calculations used in the successful semi-empirical SATIRE models at disk centre. Eventually, such a comparison should lead to the removal of the last free parameter from SATIRE-based irradiance reconstruction.

Keywords: Sun: activity; Sun: photosphere; MHD
PACS: 96.60.Mz; 96.60.Q-; 96.60.Ub

MODELLING

a) SATIRE (Spectral And Total Irradiance Reconstructions):

SATIRE has been used very successfully to reconstruct the total and spectral irradiance over the last few solar cycles [1, 2, 3]. Its underlying assumption is that all variability on time scales longer than about a day is due to changes in the solar surface magnetic fields as traced by spots, faculae and the network. The irradiance is calculated by weighting the emergent intensities of the quiet Sun, spots, faculae and network according to the number of features at a given limb angle. The emergent intensities are calculated using ATLAS9 [4] with its model for the quiet Sun, a variant of model P [5] for faculae and network, and interpolated stellar models at 4600 K and 5150 K for sunspot umbra and penumbra, respectively. The model does currently not distinguish between faculae and network, though the flux from the bright elements is scaled according to their magnetic fluxes.

Along with all currently available irradiance models, SATIRE uses 1D plane-parallel atmospheres and thus neglects changes in the shape of the flux tubes near the limb. However, despite this simple approach, there is excellent agreement between the measured and modelled total and spectral irradiance (see, e.g., [1, 3]).

CP1094, *Cool Stars, Stellar Systems and the Sun: 15th Cambridge Workshop,* edited by E. Stempels

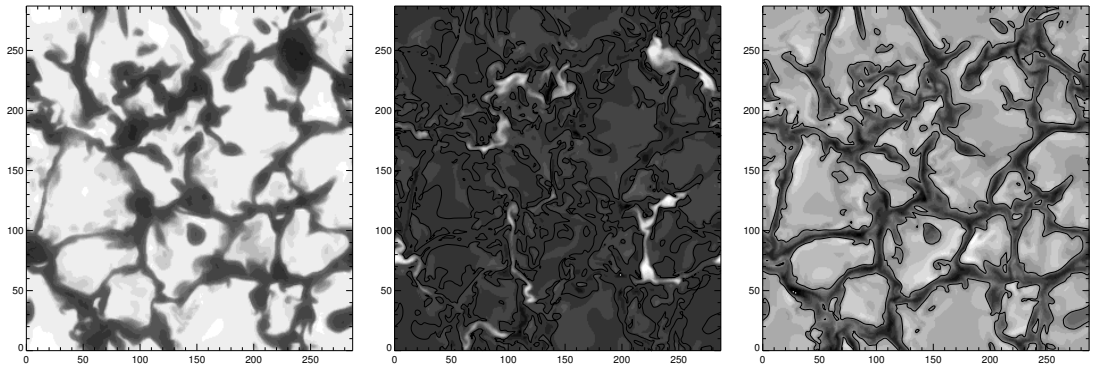

FIGURE 1. Maps of temperature, vertical magnetic field and vertical velocity at $\tau \approx 1$. The average vertical flux density was 50 G. From left to right, the grey scales are from 5000 K (black) to 11 000 K (white), from -600 G (black) to 2000 G (white) and from -10 km s^{-1} (black) to $+10$ km s^{-1} (white).

b) 3D magneto-hydrodynamic simulations:

The MURAM (MPS/University of Chicago Radiative MHD) code allows realistic simulations of solar magneto-convection in the upper convection zone and photosphere. It uses non-grey radiative transfer and open boundary conditions. It also accounts for partial ionisation and full compressibility [6]. Here we investigate 10 snapshots each for a non-magnetic comparison run, and for runs with average vertical flux densities of 50 G, 200 G and 400 G. Each simulation runs on a 288 $\times$ 288 surface grid with 100 depth points, corresponding to a solar surface area of 6$\times$ 6 Mm and a depth of 1.4 Mm. A typical snapshot with average vertical flux density of 50 G is shown in Fig. 1. As a first step we consider disk-centre intensities only, and treat each surface cell as an independent model atmosphere for which we calculate emergent intensities using ATLAS9.

RESULTS

Mean contrasts

To produce a quiet-Sun comparison spectrum, we calculate the mean intensity from the 10 non-magnetic MURAM snapshots. While the overall intensity varies for different snapshots (reflecting the solar 5-min oscillations), the spectral shape remains constant throughout. We can then investigate the effect of the magnetic field on the total output and calculate the contrasts (averaged over the whole computational box) for all snapshots. These contrasts are shown for the 200-G runs in Fig. 2 where they are also compared to the empirical SATIRE prescription. Assuming a filling factor of 20% for SATIRE, we find the SATIRE and MURAM contrasts to be remarkably similar. Note that the spectral shape of the MURAM contrasts depends strongly on the magnetic flux and typically shows steeper slopes for higher fluxes. We find that simulations with mean vertical flux densities of 400 G (shaded blue region in Fig. 2) are typically dark in the visible, but bright in the UV and IR (above $\sim 5\mu$m). At 50 G (shaded green), the contrast depends less strongly on wavelength and is generally lower than at 200 G. It is expected that the 50-G runs are more indicative of the network contrast.

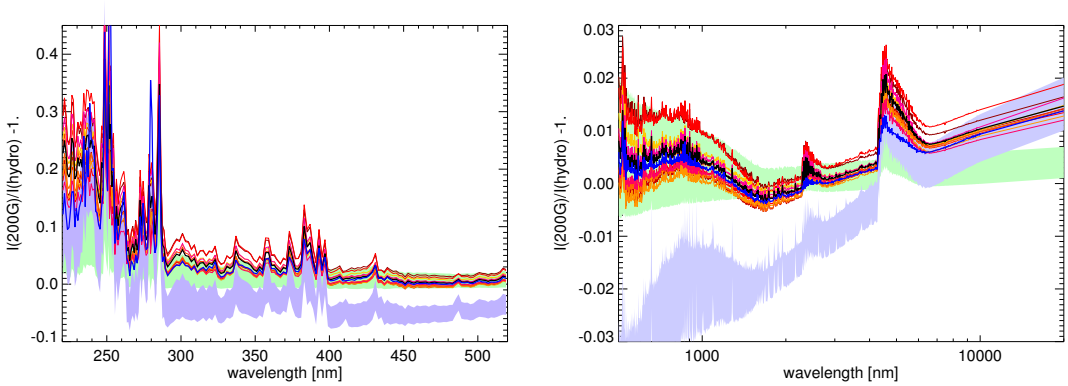

FIGURE 2. Contrast as a function of wavelength for 10 different 200G runs and averaged over the whole computational box (red lines). The average over all 10 snapshots is shown in black. The blue line is the SATIRE contrast for a filling factor of 20%. The shaded green and blue regions indicate the range of mean contrasts for average flux densities of 50 G and 400 G, respectively.

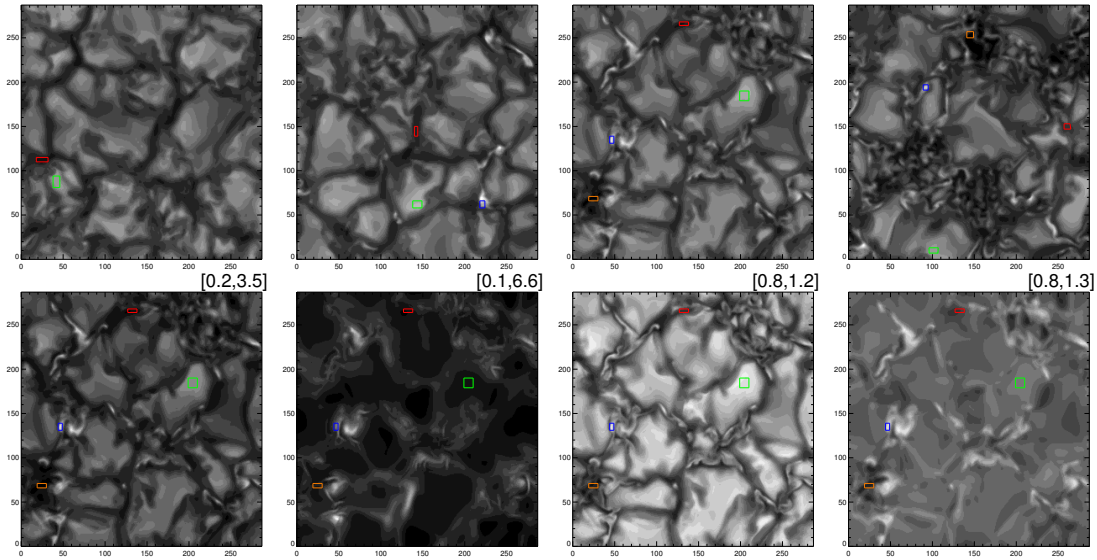

FIGURE 3. Top-row: G-band filtergrams for snapshots with average vertical flux densities of 0, 50, 200 and 400 G. The normalised intensity ranges from 0.36 (black) to 2.3 (white). Note the emergence of bright magnetic points on the three right-most images. Bottom row: filtergrams for the 200-G run with wavelength centres at 268 nm, 278 nm, 1.6 μm and 5.0 μm. The numbers in square brackets indicate the contrast values for black and white. The coloured boxes show our choices for largely field-free intergranular lanes (red) and granules (green), as well as magnetic pores (orange) and magnetic bright points (blue).

Contrasts of individual features

We can further consider the contrast of individual features compared to the overall mean of the non-magnetic runs. These features were identified on filtergrams of individual snapshots (see, e.g., the coloured boxes in Fig. 3). We distinguish between magnetic features (bright points, pores) and non-magnetic features (granules, intergranular lanes). Their contrasts at disk centre are shown in Fig. 4. The contrasts for all dark features

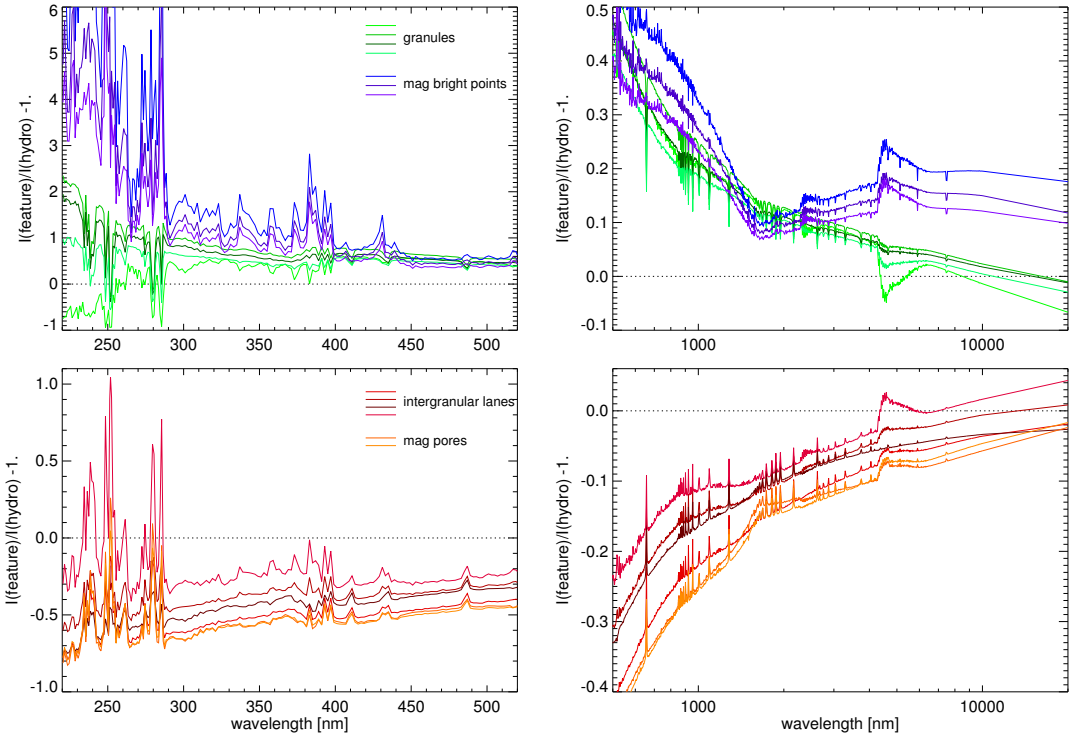

FIGURE 4. Contrasts of individual features as indicated on the snapshots shown in Fig. 3. The general colour coding is as in Fig. 3, while different colour shades are for snapshots with average vertical flux densities ranging from 0 to 400 G.

(magnetic and non-magnetic) are very similar, with only small shape changes near 1.6 μm. The spectral contrast of the bright features changes with the presence of a significant magnetic field, in particular in the UV and IR where magnetic features emit comparatively more flux. Figs 3 and 4 illustrate that magnetic bright points show up strongly in UV emission lines and generally show a steeper gradient; in the IR, they have a contrast minimum at about 1.6μm. Finally, we note that the contrast of all non-magnetic features almost vanishes near 5μm. In a next step, we will be calculating the contrast nearer the limb where such effects are expected to be much stronger.

SKS and DGA would like to acknowledge support through DFG grant SO 711/1-2 and the NERC/SOLCLI consortium grant, respectively.

REFERENCES

1. N. A. Krivova, S. K. Solanki, M. Fligge, and Y. C. Unruh, *A&A* **399**, L1–L4 (2003).
2. T. Wenzler, S. K. Solanki, N. A. Krivova, and C. Fröhlich, *A&A* **460**, 583–595 (2006).
3. Y. C. Unruh, N. A. Krivova, S. K. Solanki, J. W. Harder, and G. Kopp, *A&A* **486**, 311–323 (2008).
4. R. L. Kurucz, *Revista Mexicana de Astronomia y Astrofisica* **23**, 181–186 (1992).
5. J. M. Fontenla, E. H. Avrett, and R. Loeser, *ApJ* **406**, 319–345 (1993).
6. A. Vögler, S. Shelyag, M. Schüssler, F. Cattaneo, T. Emonet, and T. Linde, *A&A* **429**, 335–351 (2005).